Correlation Between *PTEN* and *VEGF* Expressions During the Development of Gas Gland in Japanese Eel (*Anguilla japonica*) Stimulated by Exogenous Hypophyseal Factors

Yi-Fan Chen[1], Shan-Ru Jeng[2], Ming-Chyuan Chen[3], Jin-Chywan Gwo[4], Yung-Sen Huang*[,5]

[1]*Institute of Biotechnology, National University of Kaohsiung, 700, Kaohsiung University Road, Nan Tzu Dist., 811. Kaohsiung, Taiwan*

[2]*Department of Aquaculture, National Kaohsiung Marine University, 142, Hai-Chuan Road, Nan Tzu Dist., 811. Kaohsiung, Taiwan*

[3]*Department of Marine Biotechnology, National Kaohsiung Marine University, 142, Hai-Chuan Road, Nan Tzu Dist., 811. Kaohsiung, Taiwan*

[4]*Department of Aquaculture, Taiwan National Ocean University, 2 Pei-Ning Road, Keelung 20224, Taiwan*

[5]*Department of Life Sciences, National University of Kaohsiung, 700, Kaohsiung University Road, Nan Tzu Dist., 811. Kaohsiung, Taiwan*

Abstract: Organogenesis requires support of the vascular system and control of proliferation activity. VEGF, a selective mitogen for vascular endothelial cells, is important for vessel development. PTEN, known as a tumor suppressor, regulates cell size and modulates VEGF-mediated signaling on angiogenesis. However, it is not yet clear if *PTEN* controls tissue mass by suppressing angiogenesis provoked by VEGF and their correlations in postnatal tissue development *in vivo*. We used a primitive vertebrate, Japanese eel (*Anguilla japonica*), to study this question. Swim bladder gas glands (a somatic tissue composed mainly by the capillaries) from normal eels or eels injected with hypophyseal factors were used to examine the expression of *VEGF* A, *PTEN*, *IGF*-1, and *Flk*-1 by RT-PCR. Two forms of *PTEN* (*PTEN* a, long form, and *PTEN* b, short form) cDNA have been cloned. There was no correlation between *VEGF* expression and gas gland tissue mass while a negative correlation between *PTEN* expression and tissue mass was noted; further, a higher correlation between the tissue mass and the ratio of *VEGF* to *PTEN* was shown. In summary, we have shown the involvement of VEGF and PTEN in postnatal tissue development, the ratio of *VEGF* to *PTEN* may represent the growth status of the tissue.

Keywords: VEGF, *PTEN*, *Flk*-1, *Anguilla japonica*, gas gland, *IGF*-1, development, gene expression ratio.

INTRODUCTION

Understanding how animal growth is controlled is a major topic of biology. Traditionally, the most common type of growth is coupled to cell division, and growth–increase in biomass is tightly coupled to cell–cycle progression (reviewed by [1]). Indeed, it is suggested organogenesis based on cell proliferation and multiplication requires the vascular vessels, both vasculogenesis and angiogenesis are the essential physiological processes to embryognesis, development, and somatic growth [2]; whether organ size or normal tissue mass is under the control of vascular endothelium remains an open question [3].

Vascular endothelial growth factor (VEGF), a selective mitogen for vascular endothelial cells, is an important factor for angiogenesis. VEGF is expressed at high levels close to the developing endothelium of early embryos (reviewed by [4]). Although many angiogenic factors have been identified, only VEGF makes the vascular permeable (reviewed by [5, 6]). The mRNA of VEGF is both detected in tumors and in normal tissues (reviewed by [7]). VEGF gene is highly conserved from teleost fish (Zebrafish, eel and Fugu) to mammals [8, 9]. Two VEGF receptors, Flt-1 (VEGF-R1) and *Flk*-1 (VEGF-R2, also known as KDR in humans), have been identified, both receptors have been shown to selectively expressed in vascular endothelial cells; however, only *Flk*-1 is found to mediate essential functions by VEGF stimulation, whereas VEGF-R1 expressing cells lacked such responses (reviewed by [10-12]). *Flk*-1 activates PLCγ (Phospholipase C gamma) and PI3K (Phosphoinositide 3-kinase) leading endothelial cells to become more permeable (reviewed by [13]); two isoforms of VEGF have been found in zebrafish, but only one VEGF receptor (*Flk*-1, VEGFR-2) has been reported in contrast to two VEGF receptors identified from the mammal [14, 15].

PTEN (Phosphatase and Tensin homolog on chromosome 10, also called MMAC1 or TEP1) is known to be important in both mature organism as a tumor suppressor (reviewed by [16, 17]) and embryonic development (reviewed by [18]). PTEN is a multifunctional phosphatase which lipid phosphatase activity is associated with tumor suppression [17]. The major substrate of PTEN is phosphatidylinositol-3,4,5-triphosphate (PIP3) [20]. PIP3 is produced by the action of phosphoinositide-3-kinases (PI3Ks). PI3Ks activation occurs in response to signaling induced by various growth factors (for example, insulin-like growth factors, and fibroblast growth factors) (reviewed by [17, 21]) as well as VEGF

*Address correspondence to this author at the Department of Life Science, National University of Kaohsiung, 700, Kaohsiung University Road, Nan Tzu Dist., 811. Kaohsiung, Taiwan; Tel: 886-7 5919 451; Fax: 886-7 5919 404; E-mail: yshuang@nuk.edu.tw

1874-3366/08

(reviewed by [13]). The PI3K/Akt pathway regulates cell growth, motility, and survival [22]. In endothelial cells, PI3K signaling, which is antagonized by PTEN, can mediate angiogenesis and VEGF expression [23]. PTEN negatively regulated the PI3Ks pathway and PKB/Akt activation and thus tumorigenesis [21]. It has been observed angiogenesis and *PTEN* mutations are associated with certain tumors, leading to the hypothesis these two events may be linked [24]. Actually, PTEN potently modulates VEGF-mediated angiogenesis *in vitro* [25, 26], and knockdown of *PTEN* caused an increase of pAkt leading to abnormal vasculogenesis in zebrafish *in vivo* [27]. On the other hand, PTEN is found to play a universal and profound role in normal development, since PTEN normally plays a vital role in antagonizing or in controlling the growth-promoting effects of growth factors in the developing animal (reviewed by [28]). It is suggested PTEN plays an important role in regulating cell size and growth in rodents [17] and in fruit flies [29]. But, the correlation among development, *VEGF*, *PTEN* during the postnatal tissue growth is not shown in the primitive vertebrate.

The gas gland (rete mirabile) from eels (*Anguilla* spp.) may be a good model to study the postnatal (posthatched) tissue development in vertebrates. First, the tissue mass or development of gas gland in eels is life-stage dependent, the gas gland in silver eels (pre-maturation eel) is larger than in yellow eels (immature eel) [16, 30], the same observation was also described in the eel during their sex maturation or in artificially induced matured ones [16]. Second, the gas gland is chiefly composed of endothelial cells (Krogh, 1959, cited by [31], therein), it has been demonstrated the number and density of endothelial cells in the eel gas gland were changed with its life stage or reproductive status, the number of other types cells beside the endothelial cells were reduced [9, 16, 30, 32]. Third, the phylogenic position of the eel, a member of the group of Elopomorphs considered to be close to the origin of Vertebrate evolution, may provide information on ancestral regulation in vertebrates. Based on these advantages, the development of eel tissue (gas gland) can be manipulated or controlled to study the interactions between tissue development and angiogenesis from the base of Vertebrate evolution.

The aim of this study is to examine the gene expression profile of *VEGF* and *PTEN* during posthatch (postnatal) tissue (gas gland) development in a primitive vertebrate, (*Anguilla japonica*), to see the relation among the normal posthatch tissue development and expression of *VEGF* and/or *PTEN*. Normal eels of different body sizes or eels of similar body size treated with different durations of exogenous hypophyseal factors (catfish pituitary extracts, CPE) were sacrificed, the tissue mass of gas gland was presented as RMI (gas gland somatic index = gas gland weight/ body weight x100% x 10) after calculation to normalize the data, the expression of *VEGF, PTEN* a, *PTEN* b, *IGF*-1, and *Flk*-1 in gas gland were analyzed by RT-PCR, and the correlation between gene expression and physical changes was speculated.

MATERIALS AND METHODS

1. Animals

Japanese eels (*Anguilla japonica*) were supplied by local aquafarmers. Eels of different body sizes in the same culture batch were sacrificed to get their gas gland and liver. Experimental eels (2-3 years old, body weight = 499.12 $\pm$ 58.66 g, $m \pm$ SD) with the similar body size were gradually acclimatized to seawater within two weeks just before the experiments, were randomly divided into four groups (n=6) for different treatment durations. Fish, tagged by under skin electro-magnetic tags, were kept in 6.0 M^3 (1.0 x 5 x 1.2 M) seawater re-circulating tank at 21 – 23 °C, salinity was 25 psu during experiments. Acetone preserved catfish (*Pangasius sutchi)* pituitaries (about 4.2 mg/pituitary) were provided by local aquafarmers, eels were received the dose of 2 pituitaries/kg body weight/ fish/ week, hypophyseal factors (CPE, catfish pituitary extracts) were prepared by homogenizing catfish pituitaries in saline (0.9 % NaCl solution) with glass homogenizer. Control group was received saline only. Eel received weekly injections with CPE or saline only (control group) for 9 weeks, and fish was sacrificed very 3 weeks as 3P, 6P, and 9P, respectively.

2. Cloning of eel *PTEN* cDNAs

Total RNA were extracted from eel tissues with total RNA Mini kit (Viogene Co., Taiwan). Superscript II (Invitrogen Co., USA) was used as the RT enzyme to exert reverse transcription, oligo$(dT)_{15}$ is employed as the RT-primer. The procedure is as followed in the RT official protocol (www.invitrogen.com).

The cDNA products from RT were used as template, *PTEN* degenerated primers were designed from zebrafish (NCBI accession number: CAD60625). The primer sequences are:

Forward: 5'-GATGACGTCGTTCGGTTTCTGG-3'

Reverse: 5'-GGTAATGATCCGGCTCGTTGTC-3'

The cycling program was set as follows: 95°C, 5 min (denaturing), 1 cycle only; 94°C, 30 sec (denaturing), 55°C, 30 sec. (annealing), 72°C, 50 sec. (elongating), 30 cycle; and 72°C, 5 min, 1cycle only. The PCR products were identified by their size using 1.0 % agarose gel electrophoresis. The size of the PCR products are determined by comparing it with a DNA ladder (Ultraviolet Co., Taiwan).

3. Cloning and Sequencing

The purified PCR products were subsequently ligated into a pCR-TOPO vector (Invitrogen TOPO TA Cloning Kit, Invitrogen Co., USA). The vectors were transformed in chemically competent cells (Invitrogen TOPO TA Cloning Kit, Invitrogen Co., USA). Positive transformants were determined by PCR, using primers M13F (5' GTA AAA CGA CGG CCA G 3') and M13R (5' CAG GAA ACA GCT ATG AC 3') provided by the manufacturer. PCR amplification reactions were carried out in 25 μl reaction mixtures containing 0.8 μM of each primer, 0.2 mM of each dNTP, 1.5 mM $MgCl_2$, 1 μl of the suspended clone, 0.3 U of Taq DNA polymerase (AmpliTaq, Perkin Elmer Cetus) and PCR buffer specified by the manufacturer. PCR was performed with an initial denaturation at 97°C for 5 min, followed by 30 cycles consisting of 95°C for 30 sec, 60°C for 45 sec and 72°C for 1 min, and a final extension at 72°C for 10 min.

DNA was purified from the M13-PCR product (GFX™ PCR DNA and Gel Band Purification Kit, Amersham Pharmacia Biotech Inc.). Sequencing reactions contained 4 pmol of each IRD (infrared-dye)-labelled M13 primer, 5 U of SequiTherm Excel™II DNA polymerase (Epicentre Technolo-

gies) and buffer prescribed by the manufacturer. The PCR reaction was performed with an initial denature at 95°C for 5 min, followed by 30 cycles of 95°C for 30 sec, 55°C for 15 sec and 70°C for 1 min, and a final extension at 70°C for 10 min. Subsequently, reactions were transferred to a Polyacrylamide gel in a LI-COR® automated sequencer.

4. Rapid Amplification of cDNA ends (RACE) for *PTEN*

In order to identify the 5'end as well as the 3'end of the eel *PTEN* cDNA, 5' and 3' RACE *PTEN* cDNA were performed following the instruction of the 5'/3' RACE kit (Roche Applied Science, Germany). Specific forward or reverse primers were designed from known cloned cDNA fragment (List bellowed).

PTEN a Clone Primers

Forward:5'-GATGACGTCGTTCGGTTTCTGG-3'

Reverse:5'-GACCACGCGTATCGATGTCGAC-3'

PTEN a 3'RACE

Forward:5'-GAATCCAGAGCTCGGAGCGTG-3'

Reverse: 5'-GACCACGCGTATCGATGTCGAC-3'

PTEN b 5'RACE primers

sp1:5'-CCCGTAGAAGTCGAGCGCCGTCCTG-3'

sp2:5'-AGTGGAATGGCGGCCACGTGATTGG-3'

sp3:5'-GTTGTGGTCTTCAAACGGGTACTGTGCA-3'

PTEN b 3'RACE

Forward:5'-GGCTGCTTCCTCCCCTCGAGC-3'

Reverse: 5'-GACCACGCGTATCGATGTCGAC-3'

to confirm and extent to the both ends of 5' and 3' end. The amplified DNA fragment was cloned into a pCR-TOPO vector (Invitrogen TOPO TA Cloning Kit, Invitrogen Co., USA) for subsequent sequencing.

5. Sampling Procedure

Eels were sacrificed after treatments. Following terminal anesthesia with 900 ppm 2-phenoxyethanol (Nacalai Tesque, Kyoto, Japan), the fish was dissected to get gas gland and rete mirabile somatic index (RMI = gas gland weight/body weight x 100% x10) was calculated, in the same time gas gland of each fish was sampled then total RNA was extracted by TriZol reagent (Sigma Co., USA) followed our previous work (Huang *et al*. 2006). The extracted total RNA was stored at - 80°C until the future manipulation.

6. RT-PCR (Reverse Transcription Polymerase Chain Reaction)

Reverse transcription (RT) was exerted as published [9]; in briefly, the quantity and quality of RNA was estimated by spectrophotometer (OD_{260}/OD_{280}) before RT reaction. 5 μg of RNA was employed to each RT reaction, SuperScrip II RT kits (Invitrogen Corporation, USA), and $Oligo(dT)_{15}$ were used to reverse-transcribe cDNA, the procedure is followed Invitrogen official protocol (Invitrogen Corporation, USA). The cDNA was preserved at -20°C until future assay. To analysis the expression of *VEGF*, *PTEN* a, *PTEN* b, and *Flk*-1, quantitative-PCR was performed, eel VEGF (accession number:DQ219463) specific primers (F1, R340) were followed from our previous work on eel *VEGF* [9], *PTEN* a (accession number: EF207373), *PTEN* b (accession number:EF207374), *Flk*-1 (modified from zebrafish, accession number: AAI29159), and *IGF*-1 (followed Moriyama *et al*. [33]). Specific primers for eel *cytochrome* b (accession number: AF006714) as internal standard for quantitative PCR were followed Weltzien *et al*. [34].

PTEN a PCR Primers

Forward:5'-GATGACGTCGTTCGGTTTCTGG-3'

Reverse: 5'-GCAGATTCCACACGGGTTCAG -3

PTEN b PCR primers

Forward:5'-GATGACGTCGTTCGGTTTCTGG-3'

Reverse:5'-GGTAATGATCCGGCTCGTTGTC-3'

FLK-1 PCR primers

Forward:5'-ttatcgtggaattctgcaagtatgg-3'

Reverse:5'-agaactccatgcctttagccactt-3'

IGF-1 PCR primers

Forward:5'-GAGACCCTGTGTGGGGCA -3'

Reverse:5'-TTCTGATGCACCTCCTTCTGGGTTTTG-3'

The cycling program was set as follows: 94°C, 5 min (denaturing), 1 cycle only; 94°C, 30 sec (denaturing), 53 - 56°C, 30 sec. (annealing), 72°C, 30 sec. (elongating), 25 - 35 cycles depended on different genes; and 72°C, 5 min, 1cycle only.

7. Quantification of PCR Products

The PCR products were electrophoresed on 1.0 % agarose gel at 100 V for 20 min. The PCR products were stained by Ethidium bromide (Sigma Co., USA). The size as well as intensity of the PCR products was examined by an image analysis system (Bio-1D, OnlySci. Co. Ltd., Taiwan) equipped with UV light source (CN-08, OnlySci. Co. Ltd., Taiwan). To compare the expresion level of relative genes in gas gland among different groups, the expression data were normalized by Cytochrome b and calibrated by known standard of DNA ladder markers, if the RT-PCR products from the same primers did not be run in the same gel.

8. Data Analysis and Statistics

Data were calculated and plotted as mean ± standard deviation (mean ± SD). The difference between the means of different groups were analyzed by ANOVA followed by the Student's *T*-test or multiple range *T*-test , with the level of significance in different groups set at $p<0.05$. The level of significance as well as correlation coefficient of linear regression was calculated by software SigmaPlot 2000 (SPSS Inc. Illinois, USA). Phylogenetic analysis of known *PTEN* genes was analyzed by the EMBL-EBI ClustaW (http://www.ebi.ac.uk/clustalw/).

RESULTS

1. Partial *PTEN* cDNA Sequence and Alignment

The sequencing and overlapping of the initial amplification or RACE products revealed the presence of two splice

variants of two partial *PTEN* cDNA. They comprised two partial *PTEN*-like sequences of 1039 bp (NCBI accession number: EF207373) and 967 bp (NCBI accession number: EF207374). Two splice variants of the *PTEN* gene in Japanese eel were obtained and the differences in these two *PTEN* isoforms were sketched (Fig. **1a**). Comparisons of cDNA sequence showed putative eel *PTEN* of 1039 bp had about 83 % similarity to zebrafish phosphatase and tensin homolog B (*PTEN* b; accession number: NM 001001822); further, eel *PTEN* of 967 bp had about 76 % likeness to zebrafish phosphatase and tensin-like protein B short splice variant (accession number: AY398671). Comparison of amino acid sequences deduced from the *PTEN* cDNA showed putative eel *PTEN* from 1039 bp had 87% similarity to phosphatase and tensin-like protein B long splice variant (AAR04346); on the other hand, putative eel *PTEN* from 967 bp had 83% similarity to zebrafish phosphatase and tensin-like protein B short splice variant (AAR04347). So, we named the cloned eel *PTEN* as eel *PTEN* a (long form), and the other (967 bp) as eel *PTEN* b (short form). Phylogenic analysis of known *PTEN* genes was analyzed by the EMBL-EBI. ClustaW showed a closer relation between eel *PTEN* a and zebrafish *PTEN* b, and eel *PTEN* b (short form) seemed to be more primitive and conserved during the evolution (Fig. **1b**).

2. Correlation Between Gas Gland Tissue Mass and Body Size, *VEGF*, *PTEN*, as well as the Ratio of *VEGF* to *PTEN* in Eels of Different Body Size

Eleven eels of different body size (from 44 to 1,141gram) were collected. After dissection, the correlation between body weight and gas gland tissue mass was plotted (Fig. **2a**). A curve-like pattern was found, suggesting the bigger eel (1,114 gram) had a larger gas gland (about 0.35 gram) and the smaller eel (44 gram) had a lighter gas gland tissue mass (0.02 gram). After analysis by RT-PCR, the results did not show a linear correlation (r^2=0.01) between tissue mass and *VEGF* expression (Fig. **2b**). Further, the expression of *PTEN* in different gas glands was also tested. A negative correlation (r^2=0.45) between *PTEN* expression and tissue mass was shown (Fig. **2c**). On the other hand, since the proliferation of endothelial cells is stimulated by VEGF but inhibited by *PTEN*, the gene expression ratio of *VEGF* to *PTEN* in each individual was also calculated. The results showed a positive correlation (r^2=0.47) between the ratio of *VEGF* to *PTEN* and gas gland tissue mass (Fig. **2d**). A similar manipulation was also exerted in the liver from different body size fish, the correlation coefficient (r^2) between liver mass and *VEGF*, *PTEN*, and ratio of *VEGF* to *PTEN* was 0.04, 0.001, and 0.31, respectively (data not shown here).

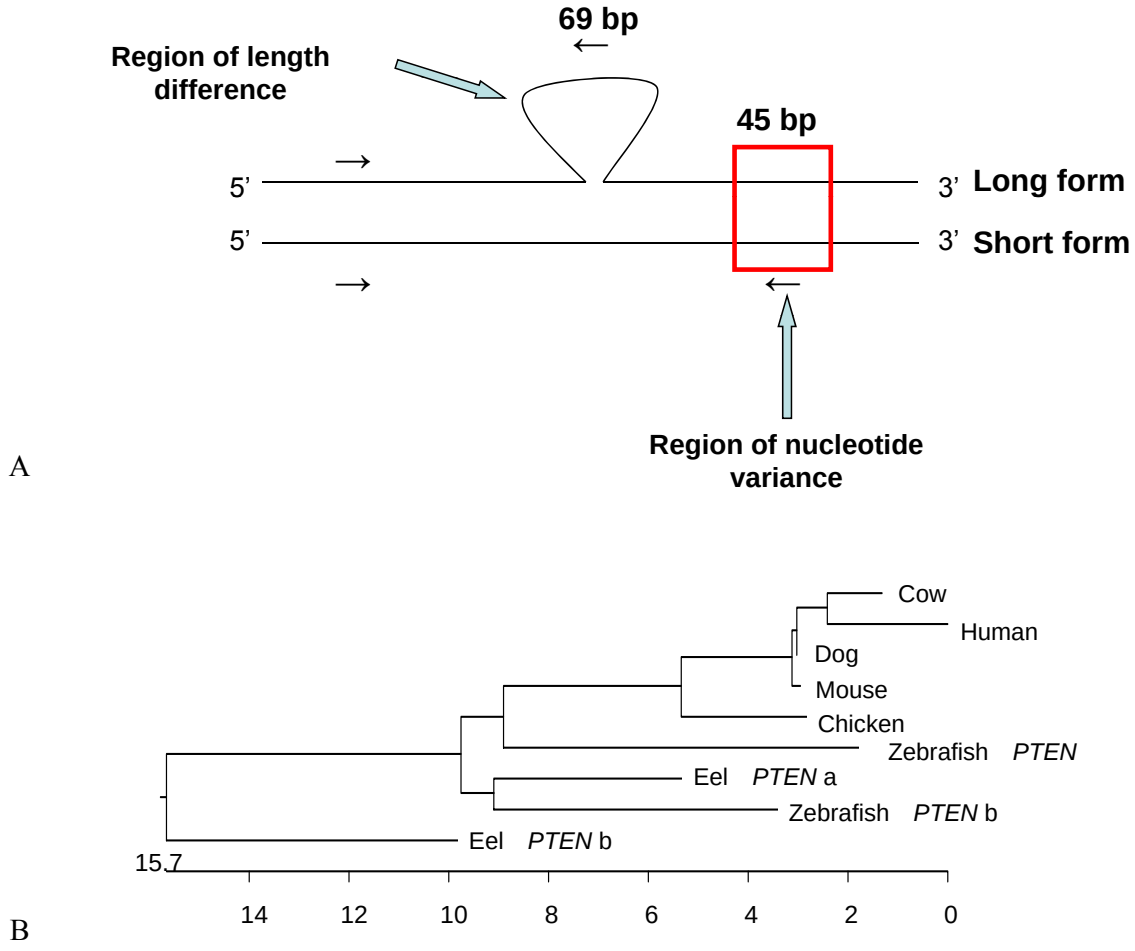

Fig. (1). Comparison of Japanese eel *PTEN* a and *PTEN* b, and phylogenic analysis. (**a**) after aligning the nucleotide sequences, the differences in two PTEN genes were indicated, the arrowheads represent the PCR primers; (**b**) dendrogram shows the phylogenic analysis of known PTEN peptide, deduced amino acid sequences were analyzed using the EMBL-EBI ClustaW. The PTEN isoform amino acid sequences of known species disclosed the teleost PTEN (zebrafish and eel) is on a separate branch compared to PTENs from other vertebrates.

3. Increase in Gas Gland Tissue Mass as well as RMI (Rete Mirabile-Somatic Index) in Eels with Similar Body Size Stimulated by Exogenous Phyophyseal Factors

Fish treated with exogenous phyophyseal factors (CPE) of different durations, 3 weeks, 6 weeks, 9 weeks represented as 3P, 6P, 9P, respectively; the control group was treated only with saline for 9 weeks represented as controls or 0P. There was no significant (p>0.05) difference in the body weight among all groups (Table **1**), on the other hand, the gas gland tissue mass or RMI (Table **1**, Fig. **3**) was significantly (p<0.05) increased after 6P compared with controls, but there was no significant (p>0.05) difference between 6P and 9P for both tissue mass and RMI (Table **1**, Fig. **3**). Gas gland tissue mass was increased x1.08 (p>0.05), x1.82 (p<0.05), and x2.56 (p<0.05) compared with controls by 3P, 6P, and 9P, respectively; RMI was also stimulated x1.06 (p>0.05), x1.77 (p<0.05), and x2.51 (p<0.05) compared with controls by 3P, 6P, and 9P, respectively.

4. Expression of *VEGF*, or *Flk*-1 in Gas Gland from Eels of Similar Body Size Affected by Exogenous Phyophyseal Factors

Analysis by RT-PCR showed the expression levels of *VEGF* under different treatment durations formed a biphasic pattern (Table **1**, Fig. **4a**). *VEGF* expression was significantly stimulated after 3P (x1.51, p<0.05, compared with controls) and 6P (x2.26, p<0.05 compared with controls) but lowered after 9P (x1.39, p<0.05 compared with controls). For double-checking the VEGF expression data, we also analyzed the expression of *Flk*-1*;* the results also showed a biphasic pattern for *Flk*-1 (Table **1**, Fig. **7b**). *Flk*-1 expression was stimulated after 3P (x6.14, p<0.05 compared with controls) and 6P (x8.85, p<0.05 compared with controls) but

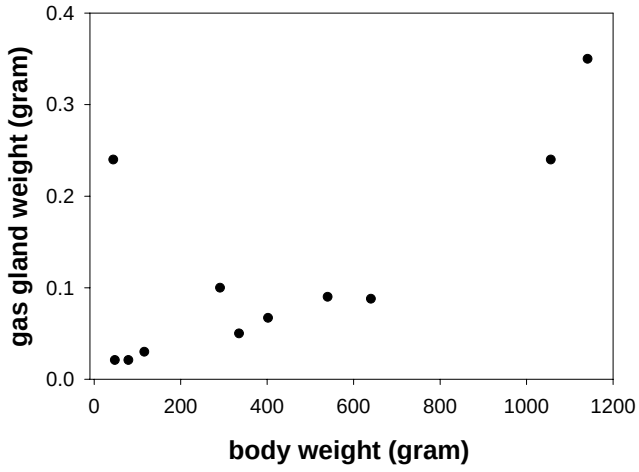

A

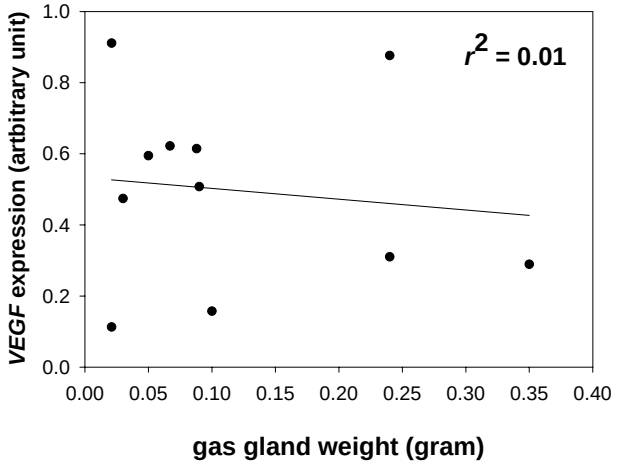

B

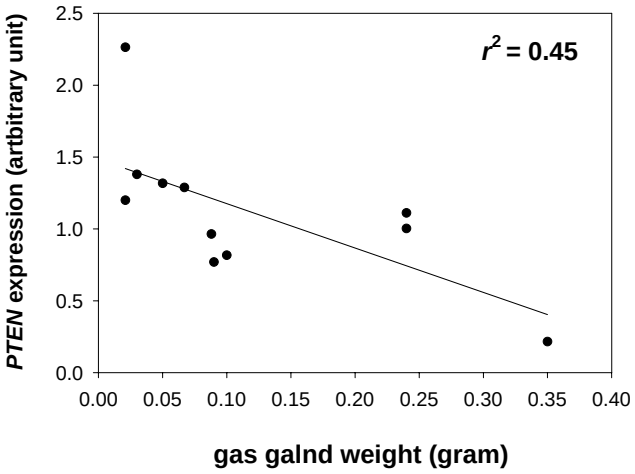

C

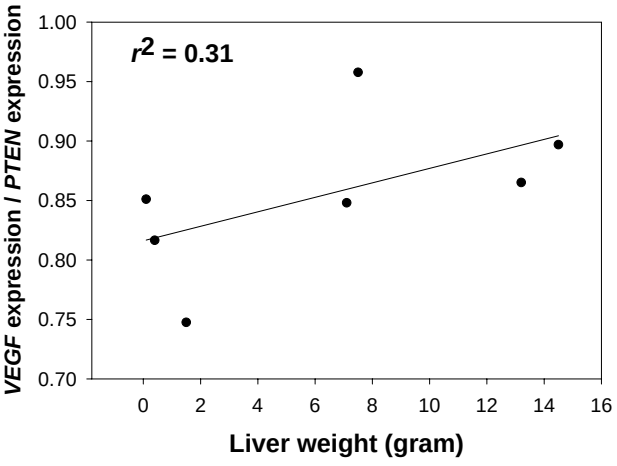

D

Fig. (2). Correlation between gas gland tissue mass and body size, *VEGF*, *PTEN* (*PTEN* b), as well as the ratio of *VEGF*/*PTEN* (*PTEN* b) in eels of different body size. Eleven eels of different body size (from 44 to 1,141gram), correlation between the tissue mass of gas gland (from 0.02 to 0.35 grams) and body size was indicated (**a**); analyzed by RT-PCR, no correlation (r^2=0.01) between tissue mass and *VEGF* expression was shown (**b**); analyzed by RT-PCR, a negative correlation (r^2=0.45) between *PTEN (PTEN* b*)* expression and tissue mass was indicated (**c**); a positive correlation (r^2=0.47) between the ratio of *VEGF*/*PTEN* (*PTEN* b) and gas gland tissue mass was noted (**d**).

Table 1.

	BW (g)	RM W (g)	RMI (10 x %)	*VEGF*	*Flk*-1	*PTEN a*	*PTEN b*	*IGF*-1
Controls	762.80±99.10 [a]	0.23±0.02 [a]	0.31±0.03 [a]	1.09±0.20 [a]	0.07±0.02 [a]	1.91±0.28 [a]	2.81±0.41 [a]	0.59±0.13 [a]
3P	767.33±74.12 [a]	0.25±0.10 [a]	0.33±0.12 [a]	1.65±0.28 [b]	0.43±0.09 [b]	1.38±0.18 [b]	2.05±0.27 [b]	0.56±0.20 [a]
6P	768.33±41.71 [a]	0.42±0.12 [b]	0.55±0.15 [b]	2.47±0.47 [c]	0.62±0.12 [c]	0.23±0.09 [c]	0.37±0.10 [c]	0.39±0.06 [b]
9P	745.20±38.38 [a]	0.59±0.24 [b]	0.78±0.27 [b]	1.52±0.16 [b]	0.04±0.02 [a]	0.02±0.00 [d]	0.18±0.04 [d]	0.45±0.08 [a]

(Data are shown as mean ± SD. Means with different letters are significantly different (p<0.05), and those with the same letter represent no significant difference. (p>0.05) within a subgroup).

dropped below the basal levels after 9P (x0.57, p>0.05 compared with controls).

5. Expression of *IGF*-1 in Gas Gland from Eels of Similar Body Size Affected by Exogenous Phyophyseal Factors

We also analyzed the expression of *IGF*-1 (insulin-like growth factor 1), known as an angiogenic factor [35, 36], in the gas gland in fish treated by different durations of CPE. The expression of *IGF*-1 in the gas gland for the different treated fish was not stimulated while *IGF*-1 expression was reduced after 6P (x0.66, p<0.05, compared with controls), then lightly increased (x0.76, p>0.05, compared with controls) (Table **1**, Fig. **4c**).

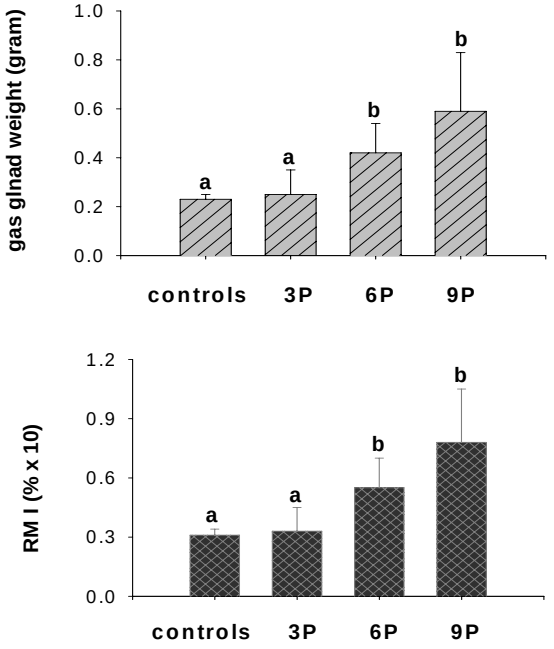

Fig. (3). Increase in gas gland tissue mass and RMI (rete mirabile-somatic index = gas gland tissue / body weight x 100% x 10) by CPE (catfish pituitary extracts). Eels received the dose of 2 pituitaries/kg body weight/ fish/ week for 3 weeks, 6 weeks, 9 weeks represented as 3P, 6P, 9P, respectively, control group was injected with saline only. Tissue mass was increased after 3P (x1.08, p>0.05), 6P (x1.82, p<0.05), and 9P (x2.56, p<0.05) compared with controls (a); RMI was stimulated after 3P (x1.06, p>0.05), 6P (x1.77, p<0.05), and 9P (x2.51, p<0.05) compared with controls (b). Data are shown as mean ± SD (n=6). The different letters are significantly different (p<0.05), and those with the same letter represent no significant difference (p>0.05) within a subgroup.

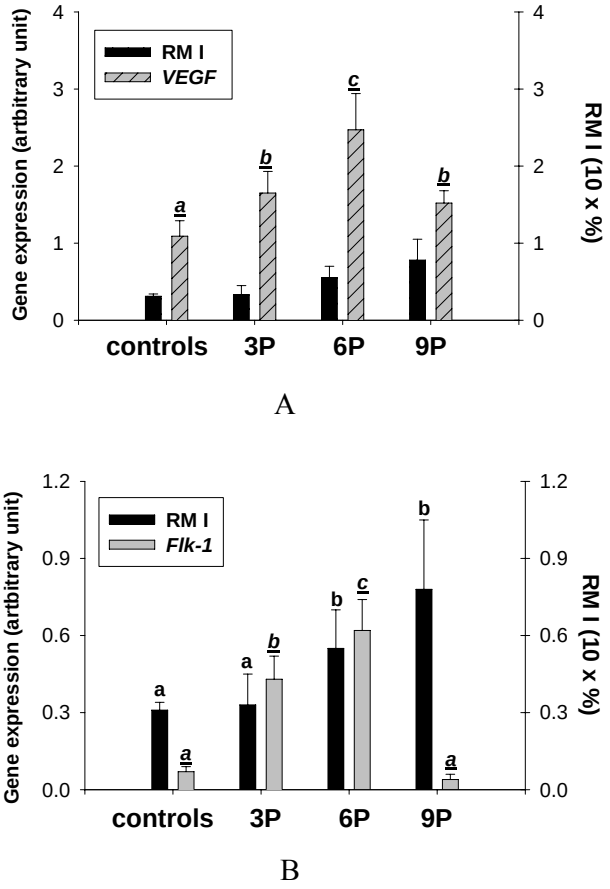

Fig. (4). Expression of *VEGF*, or *Flk*-1 in gas gland affected by CPE. *VEGF* expression was significantly stimulated after 3P (x1.51, p<0.05), 6P (x2.26, p<0.05), and 9P (x1.39, p<0.05) compared with controls, respectively, changes of RMI were also indicated (solid bar) (**a**); expression of *Flk*-1 was stimulated after 3P (x6.14, p<0.05) and 6P (x8.85, p<0.05) but drops to the basal levels after 9P (x0.57, p>0.05) compared with controls, respectively. RMI is marked as a solid bar (**b**). Data are shown as mean ± SD (n=6). The different letters significantly differ (p<0.05), and those with the same letter represent no significant difference, (p>0.05) within a subgroup.

6. Expression of *PTEN* a or *PTEN* b in Gas Gland from the Eels with Similar Body Size Affected by Exogenous Phyophyseal Factors

The expression levels of both *PTEN* a and *PTEN* b were inhibited depending on the durations of treatment (Table **1**,

Fig. **5**), the expression levels of *PTEN* a seemed lower than *PTEN* b in the same group under the same PCR condition. The expression of *PTEN* a was significantly inhibited after 3P (x0.72, $p<0.05$, compared with controls), 6P (x0.12, $p<0.05$, compared with controls), and 9P (x0.01, $p<0.05$, compared with controls). This tendency was also noted for *PTEN* b expression. *PTEN* b expression was significantly ($p<0.05$) inhibited in a time-dependent manner by the treatment. The fold on *PTEN* b expression was x0.24, x0.13, x0.06 for 3P, 6P, and 9P, compared with controls, respectively. The expression pattern of both *PTEN* a and *PTEN* b was based on different treatment durations showing a linear regression after log-scale transformation (data not shown here) between 3P and 6P for *PTEN* b or among 3P, 6P, and 9P for *PTEN* a.

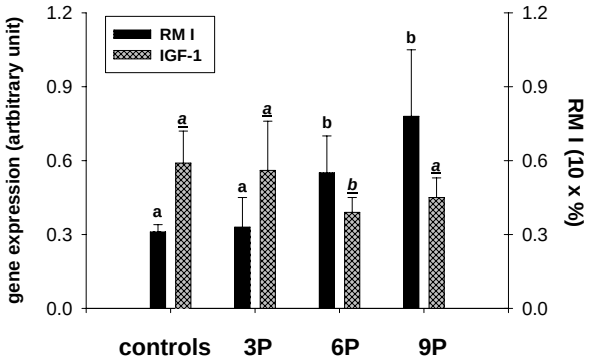

Fig. (5). Expression of *IGF*-1 in gas gland affected by CPE. Expression of *IGF*-1 was not significantly ($p>0.05$) stimulated by CPE in gas gland, *IGF*-1 expression was reduced after 6P (x0.66, $p<0.05$), then slightly increased (x0.76, $p>0.05$) compared with controls, respectively. RMI is marked as a solid bar. Data are shown as mean ± SD (n=6). The different letters significantly differ ($p<0.05$), and those with the same letter represent no significant difference ($p>0.05$) within a subgroup.

7. Correlation Among RMI (Rete Mirabile-Somatic Index) and the Ratio of *VEGF*, *Flk*-1 to *PTEN* Gene Expressions in Eels with Similar Body Size Affected by Exogenous Phyophyseal Factors

We also analyzed the correlation between the gas gland tissue mass and the ratio of *VEGF*, *Flk*-1, or *IGF*-1 to *PTEN* a or *PTEN* b. *VEGF/PTEN* a ratio was significantly ($p<0.05$) increased by x2.08, x19.67, x108.03 for 3P, 6P, and 9P compared with controls, respectively (Table **2**, Fig. **7a**). *VEGF*/*PTEN* b ratio was also significantly increased by x2.07, x18.21, x23.28 for 3P, 6P, and 9P compared with controls, respectively (Table **2**, Fig. **7a**). It seemed the trend of the increase in RMI from controls (0P) to 9P was more parallel with the ratio of *VEGF* to *PTEN* b than *VEGF* to *PTEN* a. *Flk*-1/*PTEN* a ratio was significantly ($p<0.05$) increased by x7.75, x77.75, x38.00 for 3P, 6P, and 9P compared with controls, respectively (Table **2**, Fig. **7b**). For *Flk*-1/*PTEN* b was also significantly ($p<0.05$) increased by x10.00, x87.00, x11.00 for 3P, 6P, and 9P compared with controls, respectively, (Table **2**, Fig. **7b**). *IGF*-1/*PTEN* a ratio was significantly ($p<0.05$) increased by x1.32, x6.00, x57.80 for 3P, 6P, and 9P compared with controls, respectively (Table **2**, Fig **7c**). The parallel was noted in the ratio of *Flk*-1 to *PTEN* a or *PTEN* b only among controls (0P), 3P, and 6P, this might be due to the expression of *Flk*-1 was down-regulated or autocrine-regulated by VEGF, as *VEGF* expression levels were significantly lower in 9P (x0.61, $p<0.05$, compared with 6P). *IGF*-1/*PTEN* b was also significantly ($p<0.05$) increased by x1.33, x5.83, x13.14 for 3P, 6P, and 9P compared with controls, respectively (Table **2**, Fig. **7c**). The tendency of the increase in RMI from controls (0P) to 9P was more parallel with the ratio of *IGF*-1 to *PTEN* b than 9P to *PTEN* a was. Data are shown as mean ± SD (n=6). The statistical significance of different groups, shown in Table **2**, was omitted in the figure.

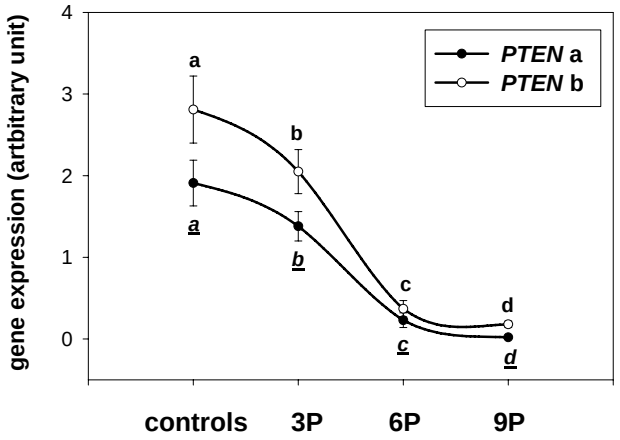

Fig. (6). Expression of *PTEN* a or *PTEN* b in gas gland inhibited by CPE. *PTEN* a expression was significantly inhibited after 3P (x0.72, $p<0.05$), 6P (x0.12, $p<0.05$), and 9P (x0.01, $p<0.05$) compared with controls, respectively. The fold on *PTEN* b expression was significantly ($p<0.05$) inhibited x0.24, x0.13, x0.06 for 3P, 6P, and 9P, compared with controls, respectively. Data are shown as mean ± SD (n=6). The different letters significantly differ ($p<0.05$), and those with the same letter represent no significant difference ($p>0.05$) within a subgroup.

Table 2.

	RMI (10 x %)	*VEGF/PTEN* a	*VEGF/PTEN* b	*Flk-1/PTEN* a	*Flk-1/PTEN* b	*IGF-1/PTEN* a	*IGF-1/PTEN* b
Controls	0.31±0.03 [a]	0.58±0.11 [a]	0.39±0.08 [a]	0.04±0.01 [a]	0.02±0.01 [a]	0.31±0.08 [a]	0.21±0.06 [a]
3P	0.33±0.12 [a]	1.21±0.18 [b]	0.81±0.11 [b]	0.31±0.08 [b]	0.20±0.05 [b]	0.41±0.12 [a]	0.28±0.11 [a]
6P	0.55±0.15 [b]	11.41±2.67 [c]	7.10±2.16 [c]	3.11±1.54 [c]	1.74±0.47 [c]	1.86±0.55 [b]	1.13±0.27 [b]
9P	0.78±0.27 [b]	62.66±6.96 [d]	9.08±2.90 [c]	1.52±0.49 [c]	0.22±0.09 [b]	17.92±2.41 [c]	2.76±0.54 [c]

(Data are shown as mean ± SD. Means with different letters are significantly different ($p<0.05$), and those with the same letter represent no significant difference. ($p>0.05$) within a subgroup).

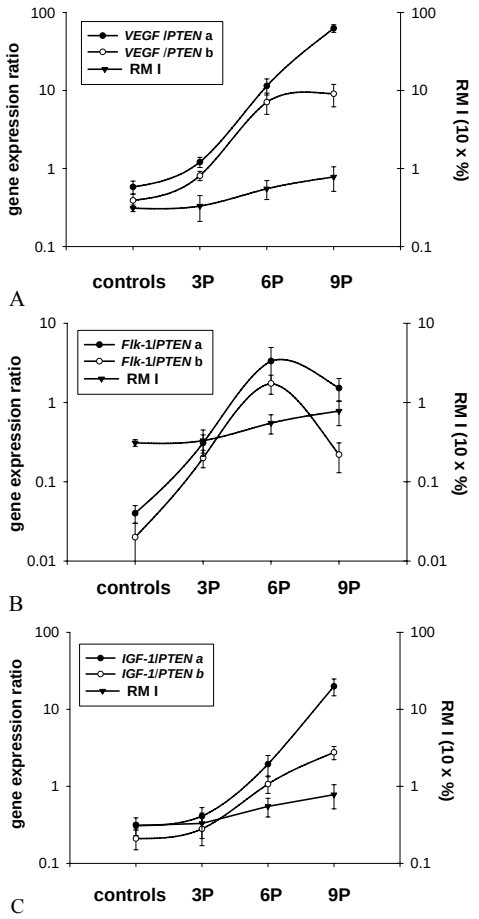

Fig. (7). Correlation among RMI (rete mirabile-somatic index) and the ratio of *VEGF*, *Flk*-1 to *PTEN* expressions affected by CPE. The ratio of *VEGF*/*PTEN* was calculated, (the value was shown in Table **2**). Ratio *VEGF*/*PTEN* a (close circle) was significantly (p<0.05) increased by x2.08, x19.67, x108.03 for 3P, 6P, and 9P compared with controls, respectively. For *VEGF*/*PTEN* b (open circle) was also significantly increased by x2.07, x18.21, x23.28 for 3P, 6P, and 9P compared with controls, respectively. The changes in RMI were also presented as reverse close triangle (a); Ratio *Flk*-1/*PTEN* a (close circle) was significantly (p<0.05) increased by x7.75, x77.75, x38.00 for 3P, 6P, and 9P compared with controls, respectively. For *Flk*-1/*PTEN* b (open circle) was also significantly (p<0.05) increased by x10.00, x87.00, x11.00 for 3P, 6P, and 9P compared with controls, respectively, RMI were presented as reverse close triangle (b); Ratio *IGF*-1/*PTEN* a (close circle) was significantly (p<0.05) increased by x1.32, x6.00, x57.80 for 3P, 6P, and 9P compared with controls, respectively. For *IGF*-1/*PTEN* b (close circle) was also significantly (p<0.05) increased by x1.33, x5.83, x13.14 for 3P, 6P, and 9P compared with controls, respectively. RMI are presented as a reverse close triangle. Data are shown as mean ± SD (n=6). The statistical significance of different groups, pointed out in Table **2**, was omitted from the figure.

DISCUSSION

The eel gas gland is mainly composed of endothelial cells (Krogh, 1959, cited by [31], therein). The interstitial space is minimal, it includes pericytes, usually between leaflets of capillaries basement membranes, and sparse bundles of collagen fibres [37]. From the specificity of its anatomical structure, the increased tissue mass of gas gland stimulated by exogenous hypophyseal factors (CPE) might be chiefly caused by the proliferation of endothelial cells. Since the capillary arrangement in gas gland changes with the life stages, the intercellular space is reduced in Japanese eel [16]. The result may give an optional answer to the question proposed in 1998 by Dr Folkman that "whether organ size or normal tissue mass is under the control of vascular endothelium?" [3]. Indeed, our preliminary work showed the increased tissue mass of gas gland was not just caused by an edema of this tissue, since a linear correlation between fresh tissue mass (wet weight) and dehydrated tissue mass (dry weight, the tissues were baked in an oven overnight at 70°C) was found (our unpublished observations). Whereas it was not known how VEGF or PTEN were involved in this process.

Two splice variants of the *PTEN* gene in Japanese eel were obtained. So far, only a single functional *PTEN* gene has been found in mammals. The major difference in these two *PTEN* isoforms is related to the region for the phosphatase folding function [27]. The minor difference was found in the C2 domain region proposed to have a potential role in membrane localization [38]. In zebrafish, the two *PTEN* genes have been demonstrated to have different functional roles in embryo development [27]. Our data suggested *PTEN* (*PTEN* b) involving the posthatched growth in eels might occur in a tissue-specific manner. A low correlation between *VEGF* expression and gas gland or liver tissue mass (r^2=0.04 or r^2=0.01, respectively) was shown. In contrast, a negative correlation (r^2=0.45) was noted between *PTEN* (*PTEN* b) expression and tissue mass in gas gland, while no correlation was noted between *PTEN* (*PTEN* b) expression and liver mass in the same animal (r^2=0.001). The lower correlation between *VEGF* expression and the mass of both tissues might be explained as follows: (1) Normally, most angiogenesis occurs during embryogenesis (reviewed by [39]), while in adult, the proliferation rate of endothelial cells is very low, with estimated turnover times from 47 to over 23,000 days [40]; (2) VEGF has been suggested to be critical during growth but to not be required for preserving the mature vasculature (reviewed by [41, 42]). In contrast, *PTEN* expression in eel runs parallel with the results obtained from humans. The fetal liver had the lowest *PTEN* level (near undetectable) while vascular endothelial cells had a high *PTEN* level during prenatal development [43]. So, in the eel, *PTEN* may play different roles in different tissues in post-hatched development. In addition, *PTEN* is shown to be constitutively active *in vivo* [44]. VEGF and PTEN might influence the eel post-hatched tissue (gas gland) development in different ways while with a converged PI3K-signaling pathway.

Because PI3K signaling mediates angiogenesis and *VEGF* expression in endothelial cells [26], and PTEN has a potent inhibitory effect on angiogenesis [21, 23, 25], we could anticipate the expression levels ratio of *VEGF* to *PTEN* (*PTEN* b) that might represent the proliferative status of endothelial cells. *VEGF*/*PTEN* (*PTEN* b) ratio showed a higher positive correlation coefficient between the *VEGF*/*PTEN* ratio and gas gland mass or liver tissue mass in eels of different body sizes (r^2=0.47, or r^2=0.31 for gas gland or liver, respectively). Actually, we don't know whether the ratio of *VEGF*/*PTEN* (*PTEN* b) always or occasionally corresponded with tissue mass, but the balance (ratio) between positive and negative factor on angiogenesis during tu-

morgenesis has been proposed or demonstrated [45, 46]. However, more data based on the expression of relative genes should be followed to reinforce this concept in the eel.

To clarify the correlation among angiogenic-related gene expressions and gas gland development, eels were treated CPE for different durations. At the same time, beside *VEGF*, the expression of *IGF*-1 (insulin-like growth factor-1), another well-known angiogenic [35, 36] and somatic growth factor [47] was noted. At the same time, expression of *Flk*-1 was also followed, the expression of *Flk*-1 might be regarded as the direct effect of VEGF on the proliferation of endothelial cells. Our results indicated the gas gland tissue mass or the RMI (the ratio of gas gland weight to body weight) was significantly increased in a time-dependent manner, but the increase in gas gland tissue mass seemed to reach a plateau between 6P and 9P. Indeed, the tissue mass of gas glands from larger normally cultured eels (body weight about 1 kilogram) is about 0.35 to 0.24 g, and 760 gram eels have a gas gland tissue mass of about 0.23 g. After CPE stimulation, the tissue mass of gas gland or RMI increases, as shown by Yamada and others in Japanese eel [16]. The biphasic pattern of both *VEGF* or *Flk*-1 gene expressions might be explained by two-stage development of the gas gland. The significant increase in gas gland tissue mass, between controls, 3P, and 6P, corresponds with significant growth of either *VEGF* or *Flk*-1 expression. Further, a mild but not significant increase in gas gland tissue mass was noted to coincide with decreased expression of both *VEGF* and *Flk*-1 between 6P and 9P. It is interesting the development of gas gland ended when the GSI (gonado somatic index = gonad weight or body weight x 100%) was superior to 3.5 % [16]. This tendency was also observed in our experiment: gas gland tissue mass or RMI did not significantly increase between 6P and 9P, coincidently, the GSI was around 3.5 % on 9P (GSI data were not shown here). The RMI fitted or corresponded with a decrease in *VEGF* expression between 6P and 9P; similar results were also noted for *Flk*-1. It is known expression of *Flk*-1 is mainly regulated by VEGF (reviewed by [10]). So, the proliferation of endothelial cells might arrest in the later stage (from 6P to 9P). This tendency is supported by the fact of VEGF is critical during growth, but is not required for preserving the mature vasculature [48]. Together, it is likely the expression of *VEGF* showed a biphasic pattern, since the development of eel gas gland is limited (near the mature status) when GSI is attended around to 3.5%, if not, hemangioma may occur.

IGF-1 expression in eel gas gland is low, which reflects to a significant extent of *IGF*-1 sequestered from the circulation (reviewed by [49]). This may explain why the expression of *IGF*-1 in the gas gland was not stimulated by CPE. But it cannot explain why the levels of *IGF*-1 expression were reduced after the 6P, since expression of *PTEN* is inhibited while VEGF is stimulated by *IGF*-1 in vascular endothelial cells (our unpublished *in vitro* data).

PTEN appears to be constitutively active *in vivo* [36], but, how to explain the lower expression levels of *PTEN* caused by CPE in the eel? The lower expression levels of *PTEN* may play certain roles to preserve the cell size in the later stage of gas gland development. *PTEN* controls the cell cycle and cell volume by different signaling transduction pathways (reviewed by [50]). The reduced PTEN activity was coupling with the PI3K-TOR (target of rapamycin) pathway in the rat [51]. Indeed, a hypothetical model of PTEN's differentiation-dependent roles has been proposed: the ability of PTEN to regulate cell growth influences the cell cycle entry of undifferentiated cells, and PTEN continues to regulate post-mitotic growth. PTEN's effects on cell growth cannot influence proliferation [50]. In summary, the decreased expression of *PTEN* leads to increased tissue mass of the gas gland, simultaneously, the lower *PTEN* leads the larger gas gland but does not become a hemangioma, although the GSI in the eel is over 3.5%.

Although we do not have any direct evidence to show if the two isoforms of *PTEN* have different physiological potencies, by correlating the RMI and the ratio of specific *PTEN* to the expression of various factors (*VEGF*, *Flk*-1, and *IGF*-1), a closer correlation between the ratio of various factors to *PTEN* b than to *PTEN* a implied the different *PTEN*s have different physiological functions. Short form *PTEN* (eel *PTEN* b) seems to play a more significant functional role in gas gland development than eel *PTEN* a did. This question may be elucidated by the gene knockdown or knockout techniques in the future.

In summary, we have shown the involvement of *VEGF* and *PTEN* in posthatched development of eel gas gland (a somatic tissue composed mainly by the capillaries) and the ratio of *VEGF* to *PTEN* may represent the growth status of the tissue. This idea fits the angiogenesis controlled by the balance or the ratio between angiogenic factors and anti-angiogenic factors [52]. Two isoforms of *PTEN*s have been identified in the Japanese eel. We postulated the physiological function of *PTEN* b, a short form, is conserved during the evolution.

REFERENCES

[1] Oldham S, Bohni R, Stocker H, Brogiolo W, Hafen E. Genetic control of size in Drosophila. Phil Trans R Soc Lond B 2000; 355: 945-952.

[2] Choi K, Kennedy M, Kazarov A, Papadimitriou JC, Keller G. A common precursor for hematopoitic and endothelial cells. Development 1998; 125: 725-732.

[3] Folkman J. Is tissue mass regulated by vascular endothelial cells? Prostate as the first evidence. Endocrinology 1998; 139: 441-442.

[4] Liang D, Chang JR, Chin AJ, *et al*. The role of vascular endothelial growth factor (VEGF) in vasculogenesis, angiogenesis, and hematopoiesis in zebrafish development. Mech Dev 2001; 108: 29-43.

[5] Ferrara N. Role of vascular endothelial growth factor in regulation of physiological angiogenesis. Am J Physiol Cell Physiol 2001; 280: C1358-C1366.

[6] Ferrara N. Vascular endothelial growth factor: basic science and clinical progress. Endocr Rev 2004; 25: 581-611.

[7] Ferrara N, Houck K, Jakeman L, Leung DW. Molecular and biological properties of the vascular endothelial growth factor family of proteins. Endocr Rev 1992; 13: 18-32.

[8] Gong BW, Liang D, Chew TG, Ge RW. Characterization of the zebrafish vascular endothelial growth factor A gene: comparison with vegf-A genes in mammals and Fugu. Biochim Biophys Acta 2004; 1676: 33-40.

[9] Huang YS, Huang WL, Lin WF, Chen MC, Jen SR. An endothelial-cell-enriched primary culture system to study vascular endothelial growth factor (VEGF A) expression in a teleostean fish, Japanese eel (*Anguilla japonica*). Comp Biochem Physiol Part A 2006; 145: 33-46.

[10] Klagsbrun M, D'Amore PA. Vascular endothelial growth factor and its receptors. Cytokine Growth Factor Rev 1996; 7: 259-270.

[11] Banerjee S, Sarkar DK, Weston AP, De A, Campbell DR. Over expression of vascular endothelial growth factor and its receptor during the development of estrogen-induced rat pituitary tumors

may mediate estrogen-initiated tumor angiogensis. Carcinogenesis 1997; 18: 1155-1161.

[12] Zachary I, Gliki G. Signaling mechanisms mediating vascular protective actions of vascular endothelial growth factor. Am J Physiol Cell Physiol 2001; 280: C1375-C1386.

[13] Olsson AK, Dimberg A, Kreuger J, Claesson-Welsh L. VEGF receptor signaling - in control of vascular function. Nat Rev Mol Cell Biol 2006; 7: 359-371.

[14] Neufeld G, Cohen T, Gengrinovitch S, Poltorak Z. Vascular endothelial growth factor (VEGF) and its receptors. FASEB J 1999; 13: 9-22.

[15] Liao W, Bisgrove BW, Sawyer H, *et al*. The zebrafish gene *cloche* acts upstream of a *flk*-1 homologue to regulate endothelial cell differentiation. Development 1997; 124: 381-389.

[16] Yamada Y, Zhang H, Okamura A, *et al*. Morphological and hisotological changes in the swim bladder during maturation of the Japanese eel. J Fish Biol 2001; 58: 804-814.

[17] Kishimoto H, Hamada K, Saunders M, *et al*. Physiological functions of Pten in mouse tissues. Cell Struct Funct 2003; 28: 11-21.

[18] Nguyen KTT, Tajmir P, Lin CH, *et al*. Essential role of Pten in body size determination and pancreatic β-cell homeostasis *in vivo*. Mol Cell Biol 2006; 26: 4511-4518.

[19] Myers MP, Pass I, Batty IH, *et al*. The lipid phosphatase activity of PTEN is critical for its tumor supressor function. Proc Natl Acad Sci USA 1998; 95: 13513-8.

[20] Maehama T, Dixon JE. The tumor suppressor, PTEN/MMAC1, dephosphorylates the lipid second messenger, phosphatidylinositol 3,4,5-trisphosphate. J Biol Chem 1998; 273: 13375-8.

[21] Hamada K, Sasaki T, Koni PA, *et al*. The PTEN/PI3K pathway governs normal vascular development and tumor angiogenesis. Genes Dev 2005; 19: 2054-2065.

[22] Thompson JE, Thompson CB. Putting the rap on Akt. J Clin Oncol 2004; 22: 4217-26.

[23] Wen SH, Stolarov J, Myers MP, *et al*. PTEN controls tumor-induced angiogenesis. Proc Natl Acad Sci USA 2001; 98: 4622-4627.

[24] Stahl JM, Cheung M, Sharma A, Trivedi NR, Shanmugam S, Robertson GP. Loss of PTEN promotes tumor development in malignant melanoma. Cancer Res 2003; 63: 2881-2890.

[25] Huang JH, Kontos CD. PTEN modulates vascular endothelial growth factor-mediated signaling and angiogenic effects. J Biol Chem 2002; 277: 10760-10766.

[26] Jiang BH, Zheng JZ, Aoki M, Vogt PK. Phosphatidylinositol 3-kinase signaling mediates angiogenesis and expression of vascular endothelial growth factor in endothelial cells. Proc Natl Acad Sci USA 2002; 97: 1749-1753.

[27] Croushore JA, Blasiole B, Riddle RC, *et al*. Ptena and Ptenb genes play distinct roles in zebrafish embryogenesis. Dev Dyn 2005; 234: 911-921.

[28] Goberdhan DCI, Wilson C. PTEN; tumor suppressor, multifunctional growth regulator and more. Hum Mol Genet 2003; 12: R239-R248.

[29] Goberdhan DC, Paricio N, Goodman EC, Mlodzik M, Wilson C. *Drosophila* tumor suppressor PTEN controls cell size and number by antagonizing the Chico/PI3-kinase signaling pathway. Genes Dev 1999; 13: 3244-3258.

[30] Kleckner RC. Swim bladder volume maintenance related to initial oceanic migratory depth in silver-phase *Anguilla rostrata*. Science 1980; 208: 1481-1482.

[31] Wanger RC, Froehlich R, Hossler FE, Handrews SB. Ultrastructure of capillaries in the red body (rete mirabile) of the eel swim bladder. Microvasc Res 1987; 34: 349-362.

[32] Bendayan M, Rasio EA. Evidence of a tubular system for transendothelial transport in arterial capillaries of the rete mirabile. J Histochem Cytochem 1997; 45: 1365-1378.

[33] Moriyama S, Yamauchi K, Takasawa T, Chiba H, Kawauchi H. Insulin-like growth factor I of Japanese eel, *Anguilla japonica*: cDNA distribution, and expression after treatment with growth hormone and seawater acclimation. Fish Physiol Biochem 2006; 31: 189-201.

[34] Weltzien FA, Pasqualini C, Vernier P, Dufour S. A quantitative real-time RT-PCR assay for European eel tyrosine hydoxylase. Gen Comp Endocrinol 2005; 142: 134-142.

[35] Lopez-Lopez C, LeRoith D, Torres-Aleman I. Insulin-like growth factor I is required for vessel remodeling in the adult brain. Proc Natl Acad Sci USA 2004; 101: 9833-9838.

[36] Froment P, Bontoux M, Pisselet C, Monget P, Dupont J. PTEN expression in ovine granulosa cells increases during terminal follicular growth. FEBS Lett 2005; 579: 2376-2382.

[37] Rasio EA, Bendayan M. Sequential morphological and permeability changers in the rete capillaries during hyperglycaemia. Microsc Res Tech 2002; 57: 408-417.

[38] Lee JO, Yang H, Georgescu MM, *et al*. Crystal structure of the PTEN tumor suppressor: implications for its phosphoinositide phosphatase activity and membrane association. Cell 1999; 99: 323-334.

[39] Risau W, Flamme I. Vasculogenesis. Annu Rev Cell Dev Biol 1995; 11: 73-91

[40] Hobson B, Denekamp J. Endothelial proliferation in tumours and normal tissues: continuous labelling studies. Br J Cancer 1984; 49: 405-413.

[41] Plank MJ, Sleeman BD. Tumor-induced angiogensis; a review. J Theor Med 2003; 5: 137-153.

[42] Yancopoulos GD, Davis S, Gale NW, Rudge JS, Wiegand SJ, Holash J. Vascular-specific growth factors and blood vessel formation. Nature 2000; 407: 242-248.

[43] Gimm O, Attie-Bitach T, Lees JA, Vekemans M, Eng C. Expression of the PTEN tumor suppression protein during human development. Hum Mol Genet 2000; 9: 1633-1639.

[44] Waite KA, Sinden MR, Eng C. Phytoestrogen exposure elevates PTEN levels. Hum Mol Genet 2005; 14: 1457-1463.

[45] Hanahan D, Folkman J. Patterns and emerging mechanisms of the angiogenic switch during tumorgenesis. Cell 1996; 86: 353-364.

[46] Fukata S, Inoue K, Kamada M, *et al*. Levels of angiogenesis and expression of angiogenesis-related genes are prognostic for organ-specific metastasis of renal cell carcinoma. Cancer 2005; 103: 931-942.

[47] Chow LML, Baker SJ. PTEN function in normal and neoplastic growth. Cancer Lett 2006; 241: 184-196.

[48] Yancopoulos GD, Davis S, Gale NW, Rudge JS, Wiegand SJ, Holash J. Vascular-specific growth factors and blood vessel formation. Nature 2000; 407: 242-248.

[49] Delafontaine P, Song YH, Li Y. Expression, regulation, and function of *IGF*-1, *IGF*-1R, and *IGF*-1 binding proteins in blood vessels. Arterioscler Thromb Vasc Biol 2004; 24: 435-444.

[50] Backman SA, Stambolic V, Mak TW. PTEN function in mammalian cell size regulation. Curr Opin Neurobiol 2002; 12: 516-522.

[51] Anand P, Boylan JM, Ou Y, Gruppuso PA. Insulin signaling during perinatal liver development in the rat. Am J Physiol Endocrinol Metab 2002; 283: E844-E852.

[52] Folkman J, ShingY. Angiogenesis. J Biol Chem 1992; 267: 10931-10934.

Received: January 09, 2008 Revised: January 22, 2008 Accepted: March 05, 2008